Modeling and Control Design for a Controllable Bearing System

D. C. Deckler, R. J. Veillette
Department of Electrical Engineering
M. J. Braun, F. K. Choy
Department of Mechanical Engineering
The University of Akron
Akron, OH 44325
USA

Abstract

This paper introduces the application of a linear-quadratic regulator to a controllable tilting-pad bearing system to reduce the vibration in a rotating machine. This application first requires a nonlinear transient simulation of the bearing to determine the stiffness and damping coefficients associated with each pad of the bearing at a given equilibrium position. The stiffness and damping coefficients are incorporated into a linear state-variable model, and a state-feedback control law is computed to minimize a quadratic performance index. The performance index parameters are adjusted to produce a suitably regulated shaft orbit in the nonlinear simulation. The results stand as a significant step toward the application of feedback control to an experimental bearing system.

1. Introduction

In all rotating equipment the shaft is primarily supported by bearings that allow it to rotate smoothly with little friction. Current rolling element and journal (sleeve) bearings are passive devices that cannot compensate for changes in their operating environment. Such changes could include lubricant contamination, viscosity changes due to thermal effects, changes in shaft speed and loading, and changes in misalignment and imbalance. An actively controlled bearing could compensate for changes in its operating environment thus leading to more stable and better-controlled shaft motion, prolonged equipment life, and increased safety.

The most common type of controllable bearing is the magnetic bearing [1,2,3]. Although appropriate for some applications, the magnetic bearing is far too costly for many low-speed, high-load applications where journal bearings excel. In addition it requires bulky and expensive power electronics and auxiliary mechanical bearings in the event of a magnetic bearing failure. The auxiliary bearings are necessary because the system is inherently unstable if the feedback control fails.

A more standard type of bearing with the potential for controllability is the tilting-pad bearing. The tilting-pad journal bearing is a fluid-film bearing in which the supporting stator sleeve is divided into segments or pads; see Figure 1. Each pad is supported on a pivot, on which it is free tilt back and forth in response to the motion of the journal. This type of bearing is known to posses excellent stability properties when used in the usual passive mode [4]. The installation of linear actuators behind the pivots would allow the application of feedback control of the radial pad positions to further improve the stability and load capacity of the system.

Ulbrich and Althus [5] were the first to present the idea of an actively controlled tilting-pad bearing. They adjusted the pads, based upon rotor speed, to obtain the necessary film thickness that optimally utilized the damping properties of a tilting pad bearing. The optimal film thickness was determined by calculation and experiment prior to the actual operation of the rotor-bearing system. Santos [6] also performed research in active tilting-pad bearings using hydraulic actuators connected to the bearing pads to move the pads to a predetermined position during or before operation of the rotor-bearing system. Although previous work has shown that the stiffness and damping coefficients of a bearing could be modified by simultaneous, equal radial movement of the pads, the use of shaft position measurements for feedback control has not been previously reported.

This paper demonstrates a linear-quadratic regulator design for active control of a tilting-pad bearing. This design constitutes a continuous feedback, which independently positions each pad to control the system dynamics without the need for determining the optimal film thickness *a priori*. A previously developed nonlinear bearing simulation [7] is first used to determine the open-loop steady-state equilibrium position of the journal in the absence of any rotor imbalance. Following [7], the stiffness and damping coefficients associated with each pad are then determined. These coefficients are incorporated into a state-variable model suitable for optimal multivariable feedback design. An optimal linear-quadratic regulator is designed and incorporated into the nonlinear simulation to determine the closed-loop response of the system. Examination of the closed-loop response allows the weighting matrices to be adjusted and the state-feedback gains recomputed to obtain a satisfactory closed-loop response. The performance index may be chosen for the regulation of the size of the journal orbit or for the reduction of the bearing forces.

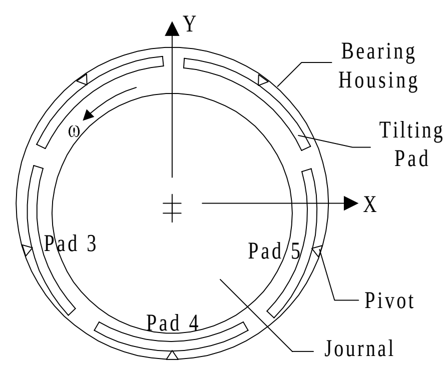

Figure 1 - A Five-Pad Tilting Pad Bearing

2. Nonlinear Closed-loop Simulation

To simulate the closed-loop journal dynamics, a nonlinear simulation of a five-pad tilting-pad bearing [7] has been modified to include a state-feedback control. The control inputs are taken to be the radial velocities of the bottom three tilting pads. At each point in time, the pad velocities are computed from the control law. The pad positions are determined by integrating the control inputs over time. Next, the pad orientation must be determined as the pads follow the movement of the journal. The appropriate pad orientation is found as the one for which the computed pressures generate a zero moment about the pivot. Once the appropriate pressures are found, they are spatially integrated to find the forces on the journal. The forces are then used in the numerical integration of the journal equations of motion. A flowchart showing the simulation structure is shown in Figure 2.

For this study, the following parameters were used:

Bearing Parameters:	Journal Parameters:
Clearance = 0.003 in	Mass = 0.2 lbs sec^2 / in
Viscosity = 0.245(10^{-5}) lbs sec / in^2	Diameter = 2.000 in
L/D ratio = 1.000	Speed = 1,000 rpm
Pad Arc = 60 degrees	Load = 10 lbs

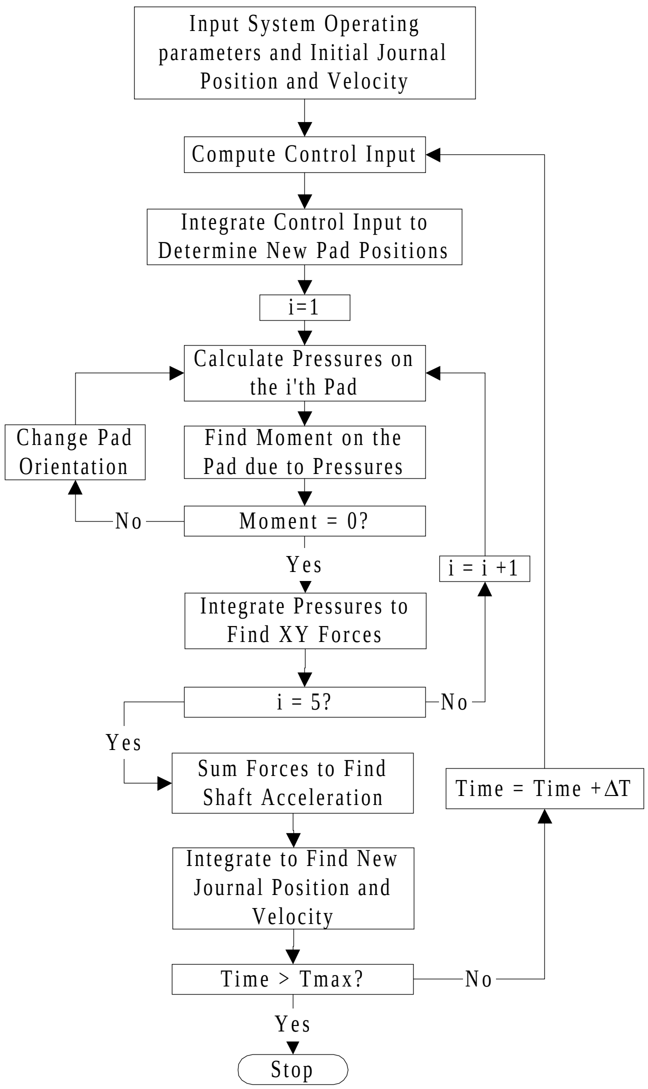

Figure 2 - Nonlinear Simulation Flowchart

The nonlinear simulation with zero assumed rotor imbalance produced a journal equilibrium position 0.81 mils directly below the center of the bearing. This equilibrium position is the operating point at which the linear model is derived.

3. Linear Model

The design of a linear feedback controller requires a linear dynamic model which approximates the behavior of the bearing at the given operating point. The nonlinear system linearized about the steady state equilibrium point takes the form

$$\delta\dot{x} = A\delta x + Bu \tag{1}$$

where δx are small position and velocity perturbations about the steady-state equilibrium point, and u is the control input vector containing the pad radial velocities. The state matrix, A, and the input matrix, B, are constant for a given set of system operating conditions. Should the operating conditions change, however, the steady state equilibrium point will change and with it the A and B matrices.

The structure of the linear control design model used for this system is shown in Figure 3. The steady state equilibrium point is the position at which the journal comes to rest when there is no imbalance present in the system. This point is obtained from the nonlinear simulation by setting the imbalance to zero and running the simulation until the journal has come to rest. The direct stiffness and damping coefficients for each pad can be determined at this position. The cross-coupled stiffness and damping coefficients are zero in a tilting-pad bearing due to the ability of the pads to follow the motion of the journal. The direct stiffness coefficients are obtained by displacing the journal a small distance δl along a radial line connecting the pad's pivot and the bearing's center and recomputing the pressures and the resulting change in force ΔF acting on the pad. The direct stiffness coefficient for the ith pad K_i is then computed using

$$K_i = \frac{\Delta F}{\delta l}. \tag{2}$$

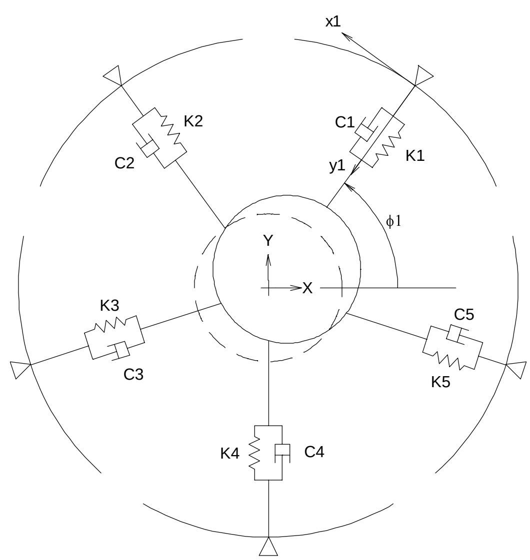

Figure 3 - Structure of the Linear Control Design Model

The direct damping coefficients are obtained by introducing a small velocity δv along a radial line and recomputing the pressures and the resulting change in force ΔF acting on the pad. The direct damping coefficient for the ith pad C_i is then computed using

$$C_i = \frac{\Delta F}{\delta v} . \qquad (3)$$

Defining the steady state equilibrium point of the journal to be the origin for a translated coordinate system $X'Y'$, the equations of motion for the journal can be written by summing the forces acting on the journal in the X' and Y' directions. Figure 4 shows these forces associated with the ith pad, where

F_{ki} = force from ith spring due to a change in journal position,
P_{ki} = force from ith spring due to a change in ith pad position,
F_{ci} = force from ith damper due to a change in journal velocity,
P_{ci} = force from ith damper due to a change in ith pad velocity.

The forces due to the journal position and velocity are

$$F_{ki} = K_i y_i' , \qquad F_{ci} = C_i \dot{y}_i' , \qquad (4)$$

where y_i' and $\dot{y}_i'$ are the radial position and velocity of the journal in ith rotated coordinate system as shown in Figure 4. The position and velocity of the journal, however, is in the global $X'Y'$ coordinate system so it is necessary to perform a coordinate transformation, which yields

$$F_{ki} = K_i(-X'\cos\phi_i + Y'\sin\phi_i)$$
$$F_{ci} = C_i(-\dot{X}'\cos\phi_i + \dot{Y}'\sin\phi_i) . \qquad (5)$$

The pad forces are simply

$$P_{ki} = K_i y_i , \qquad P_{ci} = C_i \dot{y}_i , \qquad (6)$$

where y_i and $\dot{y}_i$ are the radial position and velocity of the ith pad. Note that a journal load (assumed in the negative Y direction) is not shown in the free body diagram, since the load is taken into account in computing the equilibrium position. Also since the journal position is below the center of the bearing, the top two pads have no effect, and their stiffness and damping coefficients are set to zero.

The pad positioning actuators are modeled as integrators with the control inputs being the pad velocities. Currently there are no other actuator dynamics included in either the linear model or the nonlinear simulation.

Summing forces, the resulting system of equations takes the form given by Eq. 1 with

$$A = \begin{bmatrix} 0 & 0 & 1 & 0 & 0 & 0 & 0 \\ 0 & 0 & 0 & 1 & 0 & 0 & 0 \\ A_{31} & 0 & A_{33} & 0 & A_{35} & 0 & A_{37} \\ 0 & A_{42} & 0 & A_{44} & A_{45} & A_{46} & A_{47} \\ 0 & 0 & 0 & 0 & 0 & 0 & 0 \\ 0 & 0 & 0 & 0 & 0 & 0 & 0 \\ 0 & 0 & 0 & 0 & 0 & 0 & 0 \end{bmatrix}$$

$$\delta x = \begin{bmatrix} \delta X' & \delta Y' & \delta V_x & \delta V_y & \delta y_3 & \delta y_4 & \delta y_5 \end{bmatrix}^T$$

$$B = \begin{bmatrix} 0 & 0 & B_{31} & B_{41} & 1 & 0 & 0 \\ 0 & 0 & 0 & B_{42} & 0 & 1 & 0 \\ 0 & 0 & B_{33} & B_{43} & 0 & 0 & 1 \end{bmatrix}^T \quad u = \begin{bmatrix} \delta\dot{y}_3 \\ \delta\dot{y}_4 \\ \delta\dot{y}_5 \end{bmatrix} \qquad (7)$$

where

$$A_{31} = (-K_3\cos^2\phi_3 - K_5\cos^2\phi_5)/m$$
$$A_{33} = (-C_3\cos^2\phi_3 - C_5\cos^2\phi_5)/m$$
$$A_{35} = -K_3\cos\phi_3/m \qquad A_{37} = -K_5\cos\phi_5/m$$
$$A_{42} = (-K_3\sin^2\phi_3 - K_4 - K_5\sin^2\phi_5)/m$$
$$A_{44} = (-C_3\sin^2\phi_3 - C_4 - C_5\sin^2\phi_5)/m$$
$$A_{45} = -K_3\sin\phi_3/m \qquad A_{46} = +K_4/m$$
$$A_{47} = -K_5\sin\phi_5/m \qquad B_{31} = -C_3\cos\phi_3/m$$
$$B_{33} = -C_5\cos\phi_5/m \qquad B_{41} = -C_3\sin\phi_3/m$$
$$B_{42} = -C_4/m \qquad B_{43} = -C_5\sin\phi_5/m$$

and m is the mass of the journal.

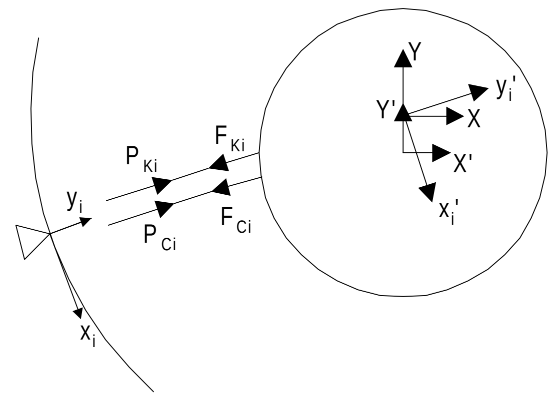

Figure 4 - Coordinate Systems and Forces for the ith Pad

4. Linear State-Feedback Design

Given a simplified linear design model of the bearing, a controller may be designed by use of standard design techniques. The design consists of determining a state-feedback control

$$u = K\delta x . \qquad (8)$$

Since the vector δx represents the complete state of the bearing model, the state-feedback control takes advantage of all the information relevant to the control of the system. The state-feedback gains K can be designed by the optimization of a performance index of the form

$$J = \int_0^\infty \begin{pmatrix} \delta x^T & u^T \end{pmatrix} \begin{pmatrix} Q & V \\ V^T & R \end{pmatrix} \begin{pmatrix} \delta x \\ u \end{pmatrix} dt . \qquad (9)$$

The controller is designed by choosing the weighting matrices Q, R, and V so that the specified design requirements are met. Once these are chosen, the state-feedback gain is found following a standard approach [8] as

$$K = -R^{-1}(V^T + B^T M) , \qquad (10)$$

where M is the positive definite solution of the matrix algebraic Riccati equation

$$\overline{A}^T M + M\overline{A} - MBR^{-1}B^T M + \overline{Q} = 0 . \qquad (11)$$

where $\overline{A} = A - BR^{-1}V^T$ and $\overline{Q} = Q - VR^{-1}V^T$.

In this study, the weighting matrices were chosen for the regulation of the journal orbit. The weighting matrices Q and R are chosen to be diagonal, and V is chosen to be zero. The initial values of Q and R were chosen as

$$Q = diag[10^4, 10^4, 1, 1, 10^4, 10^4, 10^4]$$

$$R = I_3 .$$

The weighting factors of 10^4 applied to the position state variables were chosen based on the relative amplitudes of the journal positions and velocities in the open-loop nonlinear simulation. Given the units assumed in the simulation, the velocities were approximately 100 times greater than the positions; see Figure 5. The weightings on the position variables were therefore chosen 100^2 times greater that those on the velocity variables, so that the resulting quadratic terms in the performance index would be equal in magnitude. In this way all the state variables and control inputs would be equally regulated. The elements of Q and R were then adjusted by an iterative trial-and-error process to achieve an appropriate trade-off between the size of the shaft orbit and the actuator control effort.

5. Results

To determine an appropriate controller for regulating the orbit of the journal, the weighting matrices were chosen as

$$Q = \begin{bmatrix} a\begin{pmatrix} d10^4 I_2 & 0 \\ 0 & I_2 \end{pmatrix} & 0 \\ 0 & d10^4 I_3 \end{bmatrix}$$

$$R = I_3$$

where a and d are design parameters. The following observations were made during the selection of the appropriate weighting matrix Q. The parameter a affects the penalty on the journal-related state variables relative to the pad-related variables. Increasing a causes a reduction in the shaft orbit; see Figure 6. The parameter d affects the penalty on the journal and pad displacements relative to the journal and pad velocities. Decreasing d has the effect of increasing the damping of the bearing: the shaft orbit takes longer to reach steady state; see Figures 7a and 7b.

Figures 8 and 9 show the response for a=10 and d=1. Figure 8 shows the open-loop and closed-loop shaft orbits predicted by the nonlinear simulation along with the closed-loop orbit from the linear simulation. As can be seen, the closed-loop shaft orbit is significantly smaller and more elliptical, close to that which is predicted by the linear model. In effect, the feedback control keeps the bearing system closer to a linear regime of operation. Figure 9 shows the time response of the shaft position and velocity, and the pad positions, velocities, and forces. The responses associated with the three pads have the expected phase relationships for the assumed counterclockwise rotation of the shaft.

6. Conclusions

A linear-quadratic regulator design for a five-pad controllable tilting-pad bearing was presented. Both linear and nonlinear closed-loop simulation results were shown and compared with the open-loop response. It was shown that it is possible, by means of radial movement of the pads, to reduce the orbit of the shaft and keep the bearing system close to a linear operating regime.

Future work will be aimed at the application of feedback control to an experimental tilting-pad test rig. Toward this goal, the next steps in the simulation work will include the following:

1. Incorporate in the nonlinear simulation and the linearized model the stiffness and damping characteristics of the shaft.
2. Develop and use a more detailed model of the piezoelectric actuators to move the pads of the bearing.
3. Include in the control design a linear state estimator, so that the feedback may be implemented using only the available sensors.

Experimental validation of the nonlinear simulation model and application of the feedback control in hardware will follow.

References

[1] P. Allaire, E. Maslen, R. Humphris, C. Knosp, and D. Lewis, "Magnetic Bearings," Chapter in CRC Hndbk of Lubrication and Tribology., Vol. III, E. R. Boozer Ed., 1994, pp. 577-600.

[2] E. Maslen, P. Allaire, A. Scott, and P. Hermann, "Magnetic Bearing Design for a High Speed Rotor," Proceedings of the First International Symposium on Magnetic Bearings, ETH Zurich, Switzerland, June 6-8, 1988, pp. 137-146.

[3] S. Akishita, T. Morimura, and S. Hamaguchi, "Vibration Control of Magnetically Suspended Flexible Rotor by the Use of Optimal Regulator," Proc. of the 2nd Inter. Symposium on Mag. Bearings, Tokyo, Japan, July 12-14, 1990, pp. 147-154.

[4] D. Childs, *Turbomachinery Rotordynamics Phenomena, Modeling, and Analysis*, John Wiley and Sons, 1993, p. 191.

[5] H. Ulbrich and J. Althaus, "Actuator Design for Rotor Control," Proc. of the 12th ASME Conf. Vib. & Noise, 1989, pp. 17-22.

[6] I. F. Santos, "On the Adjusting of the Dynamic Coefficients of Tilting-Pad Journal Bearings," ASME/STLE Tribology Conf., Lahaina, Hawaii, October 16-20, 1994, pp. 1-7.

[7] D. Deckler, R. Veillette, M. Braun, and F. Choy, "Modeling of a Controllable Tilting Pad Bearing," American Control Conference, Albuquerque, New Mexico, June 4-6, 1997, vol. 5, pp. 3416-3420.

[8] F. Lewis, *Optimal Control*, John Wiley and Sons, 1986, p. 203.

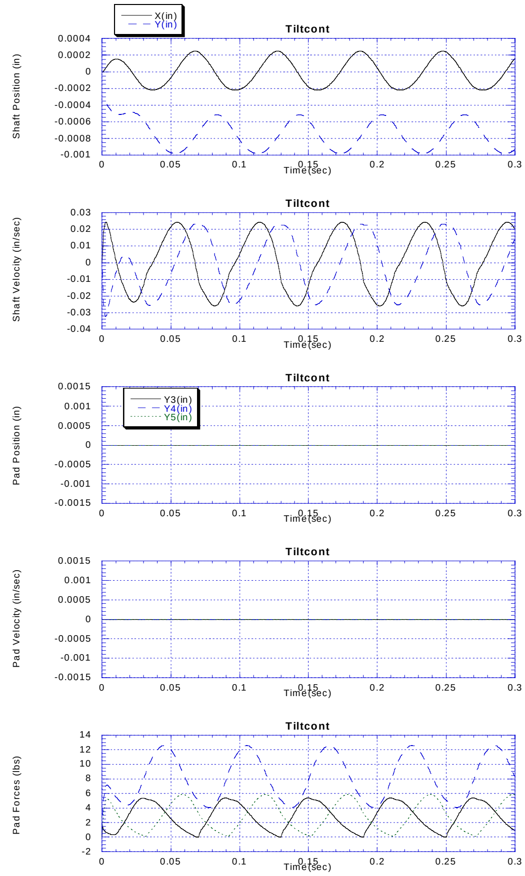

Figure 5 – Open Loop Time Responses

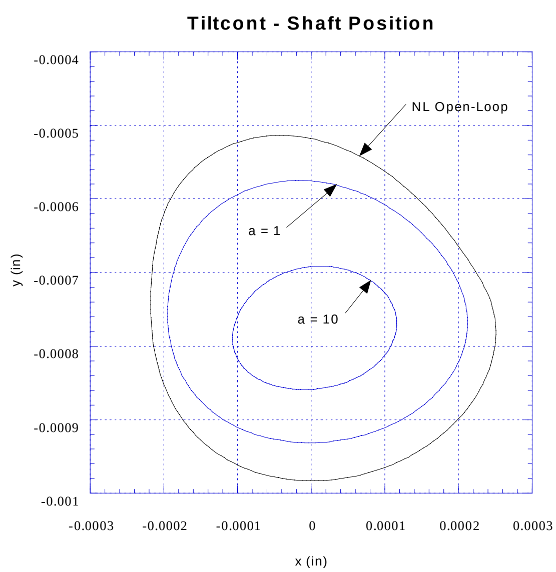

Figure 6 – Steady-State Orbits for Orbit Regulating Control with $d = 1$ and Two Different Values of a.

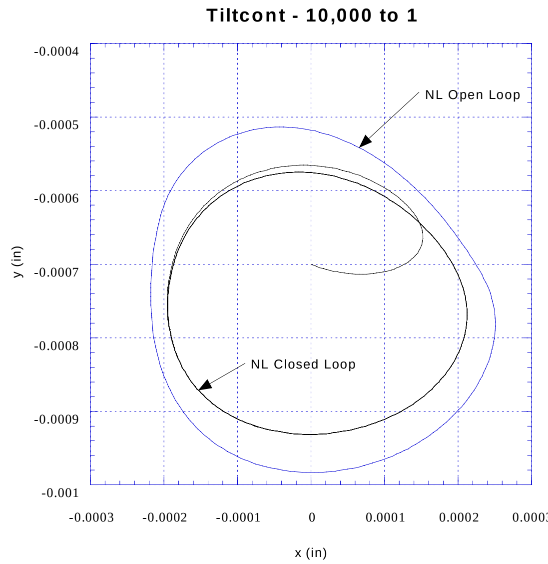

Figure 7a – Transient Response for $a = 1$ and $d = 1$.

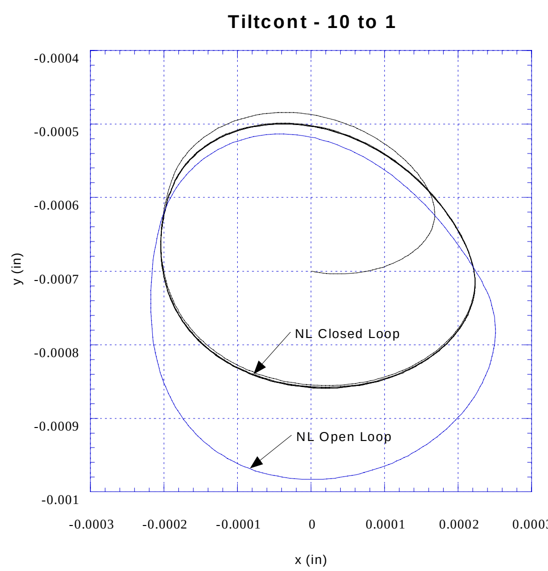

Figure 7b – Transient Response for $a = 1$ and $d = 0.001$.

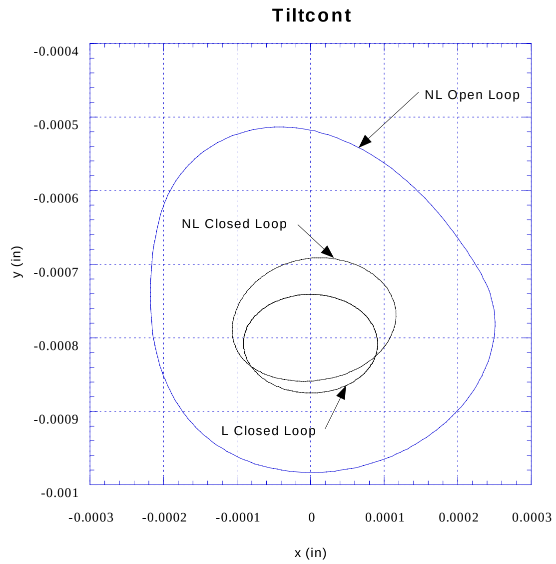

Figure 8 – Comparison of Linear and Nonlinear Closed-Loop Steady-State Response for a = 10 and d = 1.

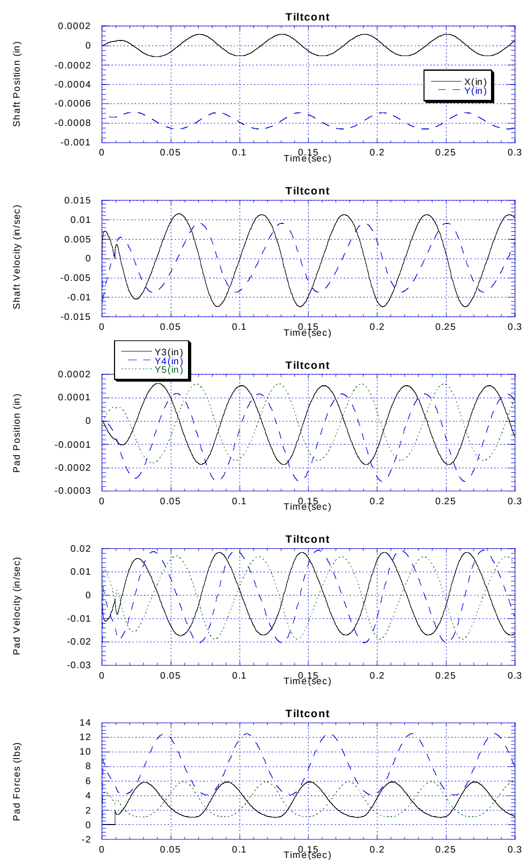

Figure 9 – Nonlinear Closed-Loop Time Responses for a = 10 and d = 1.